Multi-zone Modeling of Size-Resolved Outdoor Ultrafine Particle Entry into a Test House

Donghyun Rim
Andrew Persily
Steven J. Emmerich
William S. Dols
Lance Wallace

Engineering Laboratory, National Institute of Standards and Technology
100 Bureau Drive Gaithersburg, MD 20899

Content submitted to and published by:
Atmospheric Environment 2013
Volume 69; pp. 219-230

U.S. Department of Commerce
Dr. Rebecca M. Blank, Acting Secretary

National Institute of Standards and Technology
Patrick D. Gallagher, Director

Multi-zone modeling of size-resolved outdoor ultrafine particle entry into a test house

ABSTRACT

Airborne particle entry into buildings is important for human exposure to particles and associated health effects. The present study investigated the entry of size-resolved outdoor ultrafine particles into a test building under three different ventilation scenarios using a multi-zone airflow and contaminant transport model. Simulations of the entry of outdoor ultrafine particles into a residential test building were performed and validated with measurement data. The study results show that accurate particle deposition and penetration inputs are required to predict the time-varying particle concentrations in buildings. For closed-window conditions, both deposition and penetration have significant effects on modeling UFP transport, while deposition is more important than penetration for open-window conditions. As the window opening area increases, the filtering effect of the building envelope decreases and more outdoor particles enter the building through window openings. The study results also show that the indoor–outdoor (I-O) concentration ratio is a strong function of particle size and building operating conditions. The comparison between measurements and prediction suggests that a multi-zone particle transport model can provide insight into particle entry into buildings under various weather and building operating scenarios.

Keywords: ultrafine particles; indoor-outdoor relationship; multi-zone modeling; CONTAM

INTRODUCTION

Among the many airborne contaminants, ultrafine particles (UFP), <100 nm in diameter, are of great importance because of their association with adverse health effects such as oxidative damage to DNA (Bräuner et al. 2007; Vinzents et al., 2005) and cardiac and respiratory mortality (Stölzel et al. 2007; Oberdörster et al. 2007). In the absence of indoor sources, UFP concentrations in buildings are determined by the entry of outdoor air particles (Kearney 2011; Rim et al. 2010; Zhu et al. 2005; Long et al. 2001). Outdoor UFP originating from vehicle engines (Kittelson 1998) and atmospheric nucleation (Kulmala et al. 2004) can penetrate through the building envelope. In particular, in urban environments, entry of outdoor UFP into buildings has a significant impact on UFP levels in occupied spaces. Understanding the dynamics of urban ultrafine particle entry into a building is important for evaluating UFP exposure and the associated health effects.

Previous studies have examined transport of outdoor UFP to the indoor environments using laboratory-based or field measurements (Mullen et al. 2011; Kearney et al. 2011; Rim et al. 2010; Hoek et al. 2008; Bennett and Koutrakis 2006; Zhu et al. 2005). For example, Rim et al. (2010) found based on measurements in a test building that UFP infiltration is a function of particle size and air change rate. Other studies (Mullen et al. 2011; Kearney et al. 2011; Bennett and Koutrakis 2006; Zhu et al. 2005) monitored indoor and outdoor UFP concentrations and found that the indoor/outdoor ratio varies with particle size, building characteristics, weather conditions, season, and HVAC system operation including fan and filter usages. The studies in the literature are valuable in indentifying these important factors determining UFP entry through the building envelope; however, most of them are limited to a specific set of conditions since they are experimental studies of specific buildings in a given geographic location during a certain time period.

Outdoor conditions vary daily and seasonally while building characteristics and operation conditions also vary for different buildings, and it is a difficult task to collect indoor and outdoor UFP data in each of different buildings over long time periods. Also indoor UFP sources such as electric and gas stoves or chemical reactions are not readily controlled during experiments, complicating estimates of indoor concentrations of outdoor-originated UFP (Long et al. 2001). Given these complications, multi-zone airflow and contaminant transport modeling offers the ability to investigate transport of outdoor UFP into a building under a wide range of building operating and weather conditions. A few studies used multi-zone modeling approach to investigate the particle dynamics within buildings (Dols et al. 2011; Li et al. 2008; Sohn et al. 2007; Hu et al. 2007; Emmerich and Nabinger 2000). For example, Dols et al. (2011) investigated indoor-outdoor dynamics of fine particles for a two-story office building using the CONTAM multi-zone model, and showed the capability of the model to predict airflow and transport of fine particles by using proper model inputs. Sohn et al. (2007) simulated transport of environmental tobacco smoke (ETS) particles (0.07 μm to 1.2 μm) in a three-room multi-zone chamber using the COMIS multi-zone airflow model along with an indoor aerosol dynamics model (MIAQ4). They showed good agreement for particle size distributions (0.07 μm to 1.2 μm) between measurements and simulations. Hu et al. (2007) performed CONTAM simulation of particle resuspension due to human activities in a three-zone office building, demonstrating that the CONTAM model can be used to simulate indoor particle deposition, resuspension, and dispersion. Emmerich and Nabinger (2000) evaluated the ability of the CONTAM multi-zone model to predict concentrations of airborne particles (0.3 μm to 5.0 μm) in a residential building with the operation of two different air cleaners, considering particle deposition, penetration, and filtration efficiencies. They reported that simulated 24-h average particle concentrations were within 30 % of measurements for all particle sizes. Taken together, the previous multi-zone modeling studies have shown simulation capabilities for predicting transport behavior of airborne particles within buildings. Nonetheless, the multi-zone modeling studies in literature (Dols et al. 2011, Sohn et al. 2007, Hu et al. 2007, Emmerich and Nabinger 2000) focused on the impact of indoor sources and not on particle penetration through the building envelope. Furthermore, previous multi-zone modeling studies have rarely studied transport of UFP or nano-scale particles.

The objective of this study is to compare multi-zone modeling of indoor-outdoor UFP dynamics with actual measurement data. Such model validation is critical to ensuring that such modeling is able to provide reasonable predictions under a range of conditions, thereby supporting further model application to broader contexts. This study also develops and demonstrates a framework to simulate transient airflow and entry of ambient UFP transport into a building under different building operation and weather conditions. Using the multi-zone airflow/contaminant transport model CONTAM (Walton and Dols 2005), the present study also highlights important model input parameters and the accuracy that can be achieved in predicting the entry of outdoor UFP into a building.

METHOD

Building Description

The experimental measurements used for the model validation were conducted in a full-scale one-level manufactured test building (Nabinger and Persily 2011, see Figure 1). The test house is located on the campus of the National Institute of Standards and Technology (NIST) in the suburban Washington D.C. area, with an interstate highway within about 2 km of the test house. The outdoor UFP concentration had occasional peaks during commuting hours and in the afternoon during nucleation burst events on sunny days (Kulmala et al. 2004). The test building consists of three bedrooms, two baths, kitchen, family room, and living area, and has a floor area of 140 m^2 and a volume of 340 m^3. The exterior construction consists of insulated wood-frame walls, with exterior vinyl siding and an interior finish of vinyl covered drywall without taped and textured joints. The house is on a cinder block foundation forming a crawl space with moisture sealed walls and a floor of polyethylene sheet over crushed-stone. The crawl space has a floor area of 140 m^2 and a volume of roughly 140 m^3. The house's heating, ventilating and air-conditioning (HVAC) system consists of a 22 kW gas furnace, a 15 kW air conditioner, and a forced air re-circulation fan with a design airflow rate of 470 L/s. The leakage areas for the whole building and the air distribution ductwork were determined using whole building pressurization tests with a measurement uncertainty of about ±10 % (Nabinger and Persily 2011). These values were used in the CONTAM model of the test house as discussed later in this paper.

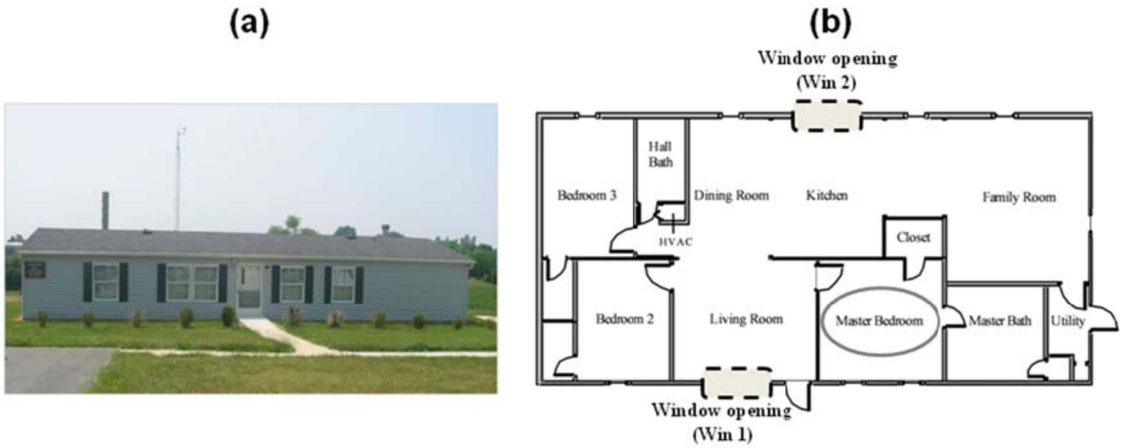

Figure 1. a) Test building; b) Floor layout of the house.

Validation Experiments

The model validation of time-varying airflow and temporal UFP transport involved a total of twelve measurements: four tests with all windows closed; four tests with one window (Win 1 in Figure 1) open 650 cm^2; two tests with two windows (Win 1 & Win2 in Figure 1) open 1300 cm^2 for each; and two tests with two windows (Win 1 & Win 2 in Figure 1) open 650 cm^2 each. Detailed conditions for each test are summarized in Table 1. Wind data (direction and speed) were collected at the top of the experiment site until July 2009, after which time the weather station was not operating properly. After that time, the weather data were collected from the weather station located on the NIST campus upon the roof of a 4-story (20 m) building approximately 1 km away from the test building. Note that the weather data that were not collected at the experiment site could impact the air change rate predictions.

Table 1. Test ID, conditions, window, temperature difference, wind speed.

Window Opening	Test ID	Test Date	Indoor conditions		Outdoor condition	
			Temp (SD[d]) (°C)	Air Change Rate (SD) (h^{-1})	Temp (SD) (°C)	Wind Speed (m/s)
All windows closed	ClosedW1	3/1/09	23.6 (0.5)	0.37 (0.05)	0.43 (1.8)	4.5 (2.4)
	ClosedW2	4/25/09	22.0 (0.6)	0.20 (0.06)	22.8 (7.9)	6.2 (1.0)
	ClosedW3	5/2/09	20.3 (0.6)	0.15 (0.02)	17.2 (1.4)	2.0 (1.3)
	ClosedW4	5/9/09	20.6 (0.5)	0.19 (0.06)	23.0 (4.0)	3.4 (1.9)
One window open 8cm[a]	1WinOpn1	9/21/08	24.3 (1.0)	0.37 (0.08)	16.6 (6.3)	2.4 (1.5)
	1WinOpn2	10/4/08	22.9 (0.5)	0.33 (0.06)	15.7 (3.4)	6.1 (0.5)
	1WinOpn3	9/6/09	19.9 (1.6)	0.48 (0.12)	21.9 (3.7)	6.5 (0.9)
	1WinOpn4	9/20/09	19.4 (0.5)	0.40 (0.21)	16.5 (5.4)	6.0 (0.6)
Two windows open 15cm[b]	2WinOpn1	10/2/10	21.4 (2.0)	0.88 (0.34)	14.0 (3.6)	6.4 (0.6)
	2WinOpn2	10/17/10	20.4 (2.7)	0.92 (0.40)	14.6 (6.4)	7.6 (1.5)
Two windows open 8cm[c]	2WinOpn3	7/15/11	24.5 (0.5)	0.87 (0.32)	23.1 (4.2)	6.3 (0.7)
	2WinOpn4	9/5/11	22.9 (0.5)	0.83 (0.44)	23.7 (2.8)	6.2 (0.8)

a. *one window open (Win1) 650 cm^2;* ***b.*** *two windows open (Win1&Win2) 1300 cm^2 each;* ***c.*** *two windows open (Win1&Win2) 650 cm^2 each;* ***d.*** *Standard Deviation*

All of the twelve tests used an identical experimental approach. Readers are referred to Rim et al. (2010) for details of the measurements and data analysis, which presents all the measurements except the tests with two windows open. However, a brief description of the experimental approach is included as follows. In the experiment, indoor and outdoor UFP ranging from 3 nm to 100 nm were alternately monitored in the master bedroom and outdoors using a Scanning Mobility Particle Sizer (SMPS). A switching valve in the UFP monitoring system alternated sampling between indoor air and outdoor air using a timing circuit. The indoor and outdoor UFP concentrations were alternately measured over an interval of 10 min each at a height of 1.5 m above the floor (indoor samples) and ground (outdoors). During each test, the house air change rate was measured using the tracer gas decay method (ASTM 2000) with the tracer gas (SF_6) injected every 4 hours. Following the injection of the tracer gas, about 20 min to 40 min were allowed for complete mixing to be achieved, and the tracer gas concentration was measured in seven rooms of the house sequentially each minute with a dedicated electron capture detector, completing a cycle of all sampling locations in 10 minutes. Based on the decay data, the air change rates were calculated using the best fit slope to a plot of the natural log of the ratio of concentration of SF_6 to the initial concentration vs. the time of the sample. The regressions were performed over an hour using seven 10-min data points at 10-min intervals and repeated in a step-wise fashion every 10 minutes. A central air distribution fan (part of the heating and cooling system) was always on during these tests to provide mixing at a rate of 2000 m^3/h, or about 6 air changes per hour. Under closed-window conditions, the tracer gas decay rates typically agree across all rooms to within 10 % RSD. When one or two windows are open, the majority of RSDs remain within 10 %; however, the zones with the open windows sometimes led to increased RSDs, but still generally within 20 %.

For each experiment, three time-varying variables were monitored: air change rate (a), indoor concentration (C_{in}) and outdoor concentrations (C_{out}). The indoor concentration (C_{in}) resulting from the entry of outdoor particles can be expressed by the mass balance equation:

$$\frac{dC_{in}}{dt} = PaC_{out} - (a+k)C_{in} \qquad (1)$$

where P is the penetration coefficient (dimensionless); a is the air change rate (h^{-1}); k is the rate of UFP deposition onto interior surfaces including ductwork and furnace filters (h^{-1}), and C_{in} and C_{out} are the indoor and outdoor UFP number concentrations ($\#/cm^3$), respectively.

The penetration coefficient (P) is the fraction of outdoor particles that enters a building with incoming air as it moves through the building envelope. Particle deposition rate (k) represents a first-order loss due to deposition of airborne particles onto building interior surfaces. Using the difference form of the mass balance model (Equation 1), the penetration coefficient (P) and deposition loss rate (k) were estimated based on minimizing the sum of squared errors that represents the difference between the modeled and measured indoor concentrations (Rim et al. 2010).

CONTAM Simulations

The test building described in the previous section was modeled using the CONTAM multi-zone air movement and contaminant transport program (Walton and Dols 2005). CONTAM is an established simulation tool for predicting airflows and contaminant concentrations in multi-zone building airflow systems. When using CONTAM, a building is represented as a series of interconnected zones (e.g. rooms), with the airflow paths (e.g. leakage sites and open doors) between the zones and the outdoors defined as mathematical relationships between the airflow through the path and the pressure difference across it. Outdoor weather conditions and system airflow rates are used to describe mass balances of air into and out of each zone, which are solved simultaneously to determine the interzone pressures relationships and resulting airflow rates between each zone, including the outdoors. These airflow rates can be calculated over time as weather conditions and system airflow rates change. Once the airflows are established, the model can then calculate contaminant concentrations over time in each building zone based on contaminant source characteristics and contaminant removal information, such as that associated with deposition and other loss mechanisms. In the present study, the CONTAM model simulated time-varying indoor-outdoor particle transport for size-resolved UFP particles, and the model results were compared to the twelve measurements performed in the test building. Figure 2 shows an image of the building in the CONTAM graphical interface, which depicts different zones, airflow paths (doors, wall joints, windows, *etc*.), and ducts on the main floor of the building. The attic and crawl space were also included in the model but are not shown in this figure. The leakage areas of the individual airflow path were determined previously (Nabinger and Persily 2011). The whole building exterior leakage expressed as effective leakage areas (ELA) at a reference pressure of 4 Pa was measured as 555 cm^2. Table S1 (See Supplementary Material) provides details of the CONTAM air leakage values for the building leakage sites expressed as ELA at 4 Pa.

The leakage values for the various building components were used as model inputs to represent the interconnectivity between outdoor and indoor spaces. The time-varying ambient weather data and outdoor UFP concentrations were also used as inputs to calculate the temporal airflow and indoor UFP concentrations in each of the building zones. The initial indoor UFP concentrations for particles from 3 nm to 100 nm were set using a lognormal distribution (geometric mean: 50 nm, standard deviation: 1.5, total number: 860 cm^{-3}) based on a number of indoor UFP observations in the test building. However, the initial concentration inputs affected the model prediction for only the first few hours (< 3 h) and did not impact the prediction for the later simulation period. The calculation time step of the model was 30 seconds; however, given that the time resolution of the measurements was 2.5 min, the model results and the measurement data were compared at this same 2.5 min interval.

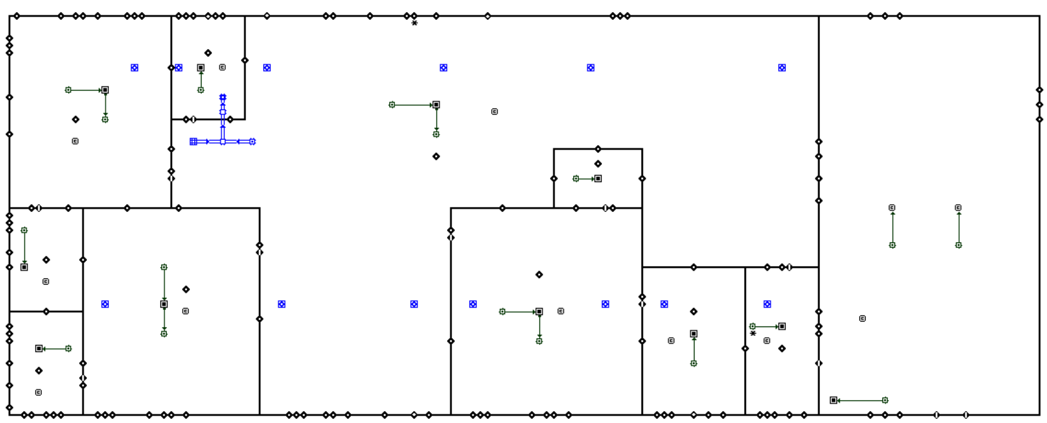

Figure 2. Graphic interface for the main floor of the test building

Two key parameters that impact indoor-outdoor UFP dynamics are particle deposition rate and penetration factor. The determination of particle deposition rates has been handled differently in previous studies. Dols et al. (2011) used the terminal settling velocity of 1 μm particles as a model input and showed that the model results agree with the average deposition values measured using small glass vials. Sohn et al. (2007) directly calculated the particle deposition using an analytical model from Nazaroff and Cass (1990). Hu et al. (2007) used mean deposition velocity of 12 μm particles (with a density of 1.3 g/cm^3), which they measured in laboratory experiments, as a deposition input in the model. Emmerich and Nabinger (2001) used deposition rate based on particle decay measurement for use in a CONTAM model to predict the performance of air cleaner. In this study, we used regression data from average measured deposition rates based on 25 experiments with the central mixing fan operating, including the twelve test cases described above and listed in Table 2 (Rim et al. 2012). These deposition values are up to five times greater than the theoretical estimates for surface deposition based on Lai and Nazaroff (2000) due to forced air re-circulation through the central mechanical fan during the measurement. The high air recirculation through the central HVAC system and ductwork led to relatively high measured UFP deposition rate (0.28 h^{-1} to 4.46 h^{-1} as seen in Table 2). Previous experimental studies also found relatively high values of UFP under central fan operation. For example, Wallace at al. (2004) reported rates of 0.8 h^{-1} to 5.0 h^{-1} for particle sizes between 10 nm and 100 nm, while He et al. (2005) estimated rates between 2.0 h^{-1} and 5.0 h^{-1} for the UFP size range from 10 nm to 100 nm.

With regard to UFP penetration into a building, most of the multi-zone modeling studies in literature (Dols et al. 2011, Sohn et al. 2007, Hu et al. 2007) explored the impact of indoor sources on indoor particle concentrations and therefore did not consider particle penetration through the building envelope. In the present study, we used average penetration coefficients (P) observed from nine different measurements with all windows closed (Rim et al. 2010). We regressed the measurement data to generate the following relationship between penetration coefficient (P) and particle diameter (D_p):

$$P = 0.14(0.01)\ln(D_p) - 0.048(0.039) \qquad (2)$$

In the equation, the numbers in the parentheses are the standard errors of the estimates of the slope and intercept. The size-resolved penetration coefficients derived using equation (2) (see Table 2) were somewhat different from theoretical penetration model of Liu-Nazaroff (2001). For example, the P values for an ideal rectangular crack with dimensions 1.0 mm high by 10 cm long at a pressure difference of 4 Pa are 0.10 and 0.93 for 10 nm and 100 nm particles, respectively. The values of P for these two particle diameters in Table 2 are 0.28 and 0.62. Possible explanations for this discrepancy are variation of indoor-outdoor pressure difference over time and rough and irregular cracks in real building that are of unknown shape, length, and height. However, the *P* values in Table 2 are comparable to experimental studies in the literature. For instance, Zhu et al. (2005) observed the mean values of 0.1 to 0.6 for particle sizes ranging from 10 nm to 100 nm) for four apartments close to a major freeway in Los Angeles, CA. Along with the size-resolved penetration coefficients for air leakage paths associated with cracks and other small openings, we assumed a penetration coefficient (*P*) of 1 for the airflow through open windows.

The size-resolved deposition loss rates (*k*) and penetration coefficients (*P*) shown in Table 2 were used as model inputs in the CONTAM simulations of indoor-outdoor UFP dynamics. Note that the penetration and deposition characteristics can vary substantially with building design, crack shape, envelope leakage area, indoor surface area, indoor-outdoor pressure differential, and building operating condition. The CONTAM model can easily consider variations in input data of deposition, penetration, and air leakage characteristics and analyze the effect of changes in the value of each parameter on the model prediction of indoor-outdoor UFP dynamics.

Table 2. Size-resolved *P* and *k* observed in the test building.

Particle diameter (nm)	Deposition loss rate (*k*) (h^{-1})	Penetration coefficient (*P*)
3.4	4.46	0.13
4	3.90	0.15
4.78	3.37	0.18
5.73	2.90	0.20
6.85	2.51	0.23
8.2	2.16	0.26
9.82	1.86	0.28
11.8	1.60	0.31
14.1	1.38	0.33
16.8	1.20	0.36
20.2	1.03	0.39
24.1	0.89	0.41
28.9	0.77	0.44
34.6	0.66	0.46
41.4	0.57	0.49
49.6	0.49	0.51
59.4	0.42	0.54
71	0.36	0.57
85	0.31	0.59
100	0.28	0.62

Statistical Analysis

The predictions of time-series data for 24-h particle concentrations were compared to the measured values using ASTM D5157 Standard Guide for Statistical Evaluation of Indoor Air Quality Models (ASTM 2003). ASTM D5157 provides three statistical tools for evaluating the accuracy of IAQ predictions and three additional statistical tools for assessing bias. The first three parameters are correlation coefficient (*r*), regression slope (*M*), and regression intercept (*b*). These parameters are related to the goodness of fit of a linear plot of the measurement and simulation results. A line with a slope of 1.0, intercept of 0.0, and a correlation coefficient of 1.0 would indicate perfect agreement between measurements and model predictions. Three additional parameters included in ASTM D5157 are normalized mean square error (NMSE), fractional bias (FB), and fractional bias of variance (FS):

$$NMSE = \overline{(C_p - C_o)^2} / (\overline{C_p}\,\overline{C_o}) \qquad (3)$$

$$FB = 2(\overline{C_p} - \overline{C_o}) / (\overline{C_p} + \overline{C_o}) \qquad (4)$$

$$FS = 2(\delta_{Cp}^{\ 2} - \delta_{Co}^{\ 2}) / (\delta_{Cp}^{\ 2} + \delta_{Co}^{\ 2}) \qquad (5)$$

C_o and C_p are the measured and predicted concentrations respectively and δ^2 is the variance. Note that normalized mean square error (*NMSE*) is zero when there is perfect agreement and tends toward higher values as measurement and prediction differ by larger magnitude. Fractional bias (*FB*) provides a normalized range of values between 2 and -2 with a value of zero corresponding to perfect agreement between measurement and prediction. Fractional bias based on the variance (*FS*) of the concentration is zero for perfect agreement.

ASTM D5157 contains the following criteria for assessing agreement between measurements and predictions:

1) The correlation coefficient (r) ≥ 0.9;

2) The line of regression between the predictions and measurements should have a slope (M) between 0.75 and 1.25;

3) An intercept (b) less than 25 % of the average measured concentration;

4) The normalized mean square error (NMSE) ≤ 0.25;

5) Absolute values of normalized or fractional bias (FB) of the mean concentrations ≤ 0.25; and

6) Absolute value of fractional bias based on the variance (FS) < 0.50.

These criteria were used to evaluate the ability of the CONTAM model to predict the indoor concentrations of UFP.

RESULTS AND DISCUSSION

This section consists of the four major parts. The first part presents the results with air change rates and total UPF concentrations. The second part provides details of size-resolved UFP concentrations depending on window position as well as a summary of statistical analysis. The third part consists of comparison of measured and predicted indoor-outdoor UFP concentration relationship and parametric analysis by considering variations in deposition rate and penetration coefficient. Finally, the fourth part provides study limitations and future implications.

Air change rates and total UFP concentrations: simulation vs. experiment

Figures 3a-3f present the measured and predicted UFP concentrations and air change rates for selected test cases under different window opening conditions. The figures show time-varying air change rates as well as indoor and outdoor UFP concentration profiles over 24-h. The figures indicate that prediction of air change rate agrees very well with the measurements with all windows closed (Figure a) and with only one window open (Figure c). The prediction is less accurate for the tests with two windows open (Figures e). This reduced accuracy seems likely due to the CONTAM airflow model assumption of quiescent or still air in a zone (Chen 2009; Wang and Chen 2008). This simplification might cause errors in the prediction of the airflow rates through large openings, especially when the momentum effect is high due to strong outdoor wind. However, even though there are uncertainties with the prediction of temporal airflow rates, the time-averaged air change rate is reasonably predicted.

Figures 3b, 3d, and 3f compare observed and predicted total UFP (3 nm to 100 nm) concentrations in the master bedroom. The results demonstrate that the indoor concentration profile follows the variation in the outdoor concentration but at a reduced level due to filtering effect of the building envelope. The measurement results show that outdoor UFP concentration is up to approximately ten times higher than the indoor concentration. Note that the dashed lines for different simulation results (Lines A, B and C) in the figures represent prediction of indoor UFP concentrations for different handling of deposition and penetration: Line A represents the results considering neither particle deposition nor penetration; Line B considers only deposition; and Line C considers both deposition and penetration. Therefore, the figures reveal differential effects of penetration loss and deposition in predicting time-varying indoor UFP concentration. Figure 3b suggests that for the case of closed windows, ignoring either penetration loss or deposition in the simulation can result in significant errors for model estimates of time-varying UFP concentrations. However, the effect of penetration loss dramatically decreases as window opening area increases (Figure 3d and 3f). For example, when two windows are open, consideration of penetration loss in addition to deposition only minimally improves the model prediction (Figure 3f). This result can be explained by the fact that as the airflow path opening area increases, the particle filtering effect of the building envelope becomes less significant compared to closed window conditions.

Table S2 (See Supplementary Material) provides airflow rates through the two windows (Win1 and Win2) and average fractions of the total airflow into the building through the two windows. According to Table S2, the average fractions of the total airflow into the house through the two windows (Win1+Win2) were predicted to be approximately 10 % for all windows closed, 75 % for one window open (Win1), and 98 % for two windows open (Win1 and Win2). The actual fractions of total UFP entering through the two windows are also about 10 % for closed window (since *P* was applied equally to all air leakage sites), higher than 75 % for one window open (since a *P* value of 1 is applied only to open window), and nearly 100 % for two windows open.

Based on the results in Figures 3a-3f, both deposition and penetration need to be taken into account for accurate modeling of time-varying indoor concentrations. Particularly for cases with closed windows, deposition and penetration losses are equally important for modeling of UFP dynamics in a building, while deposition is more significant than penetration for open window cases.

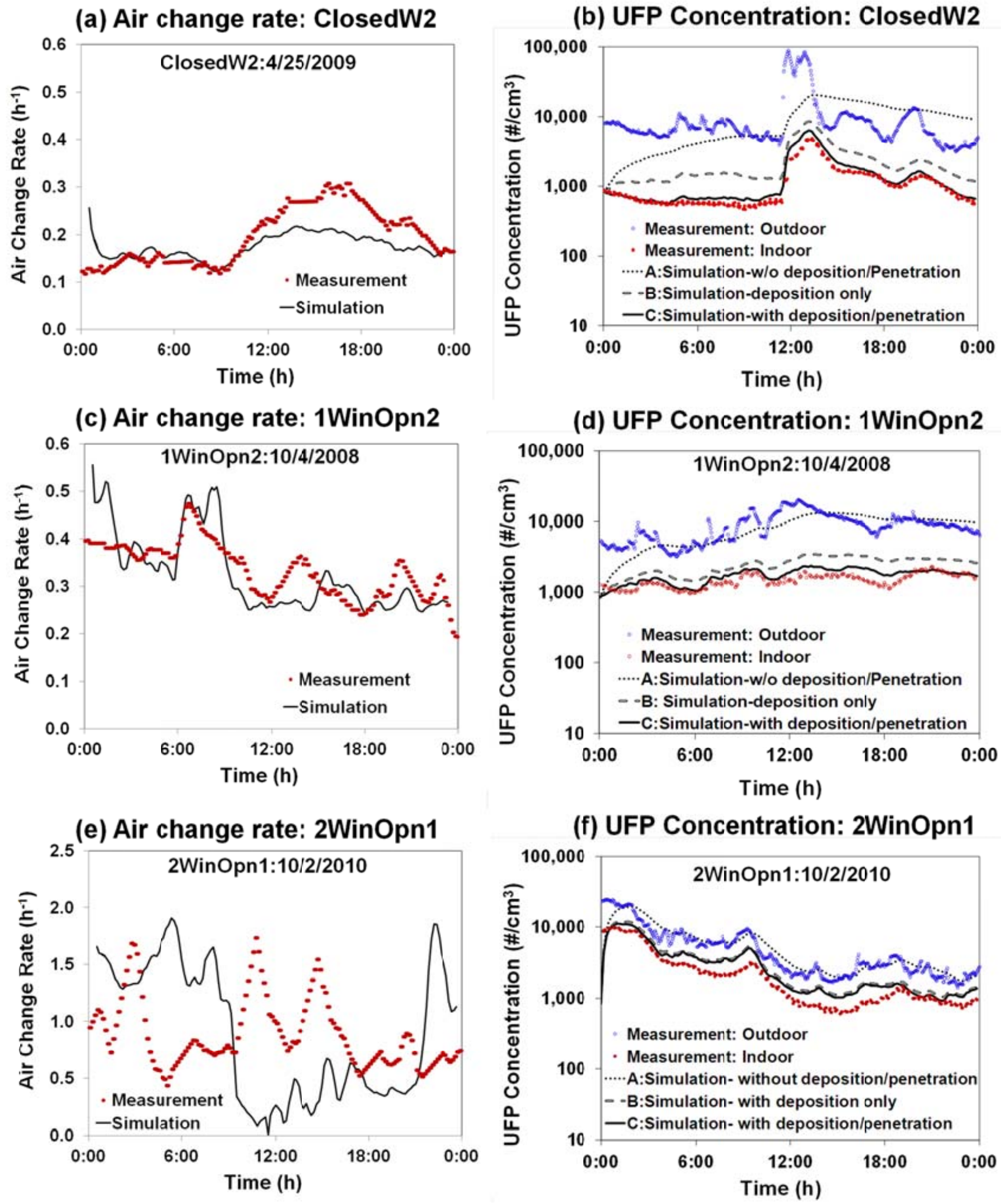

Figure 3. Measurements vs. CONTAM predictions for air change rate (a, c, and e) and total UFP concentration (b, d, and f) under three window opening conditions: all windows closed (ClosedW2, figures a-b); One window open (1WinOpn2, figures c-d); Two windows open 1300 cm^2 each (2WinOpn1, figures e-f). The y-axis is log-scale and starts from 10 instead of zero.

Size-resolved UFP Concentrations

Closed windows

Figures 4a-4d provide 24-h concentration profiles for different particle sizes (100 nm, 60 nm, 40 nm, and 20 nm) with all windows closed (ClosedW2). The measurement results show that the indoor concentration profile follows the outdoor profile with a time lag. In general, outdoor particle concentrations are higher for smaller particles, with the indoor concentrations generally the lowest for the smallest particle sizes. This trend demonstrates that particle removal across (penetration) and within (deposition) the building is largest for smallest particles.

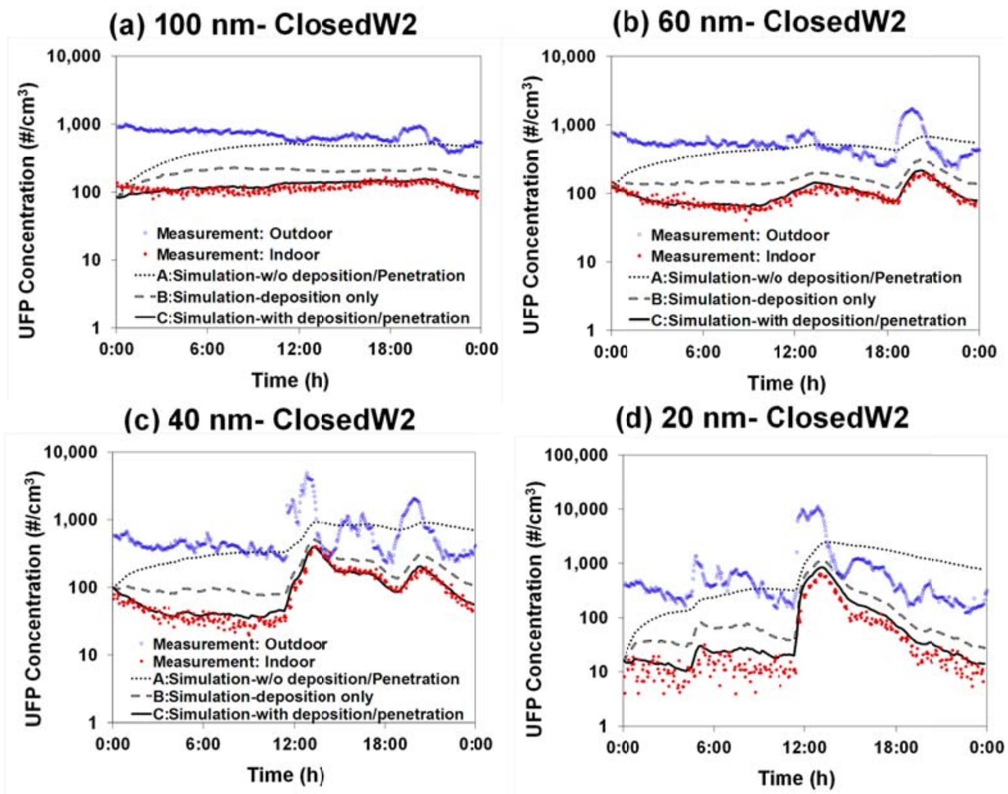

Figure 4. Time-varying (24-h) particle concentration profiles – measurement vs. simulation for the test ClosedW1: (a) 100 nm, (b) 60 nm, (c) 40 nm, and (d) 20 nm. The simulation results are varied depending on the consideration of penetration and deposition.

Given that both UFP penetration and deposition losses are important for UFP transport, Figures 5a-5f present comparisons of the model prediction and measurement for closed window conditions. The figures indicate that model performance is relatively good for the range of particle sizes. The model predicts temporal changes in particle concentration with reasonable accuracy. The prediction is least accurate for the smallest particle size (20 nm). In this case, the discrepancy likely exists because small particles are very sensitive to local airflow and environmental conditions, and the model might not catch all the details of the dynamics of small particles at local scale.

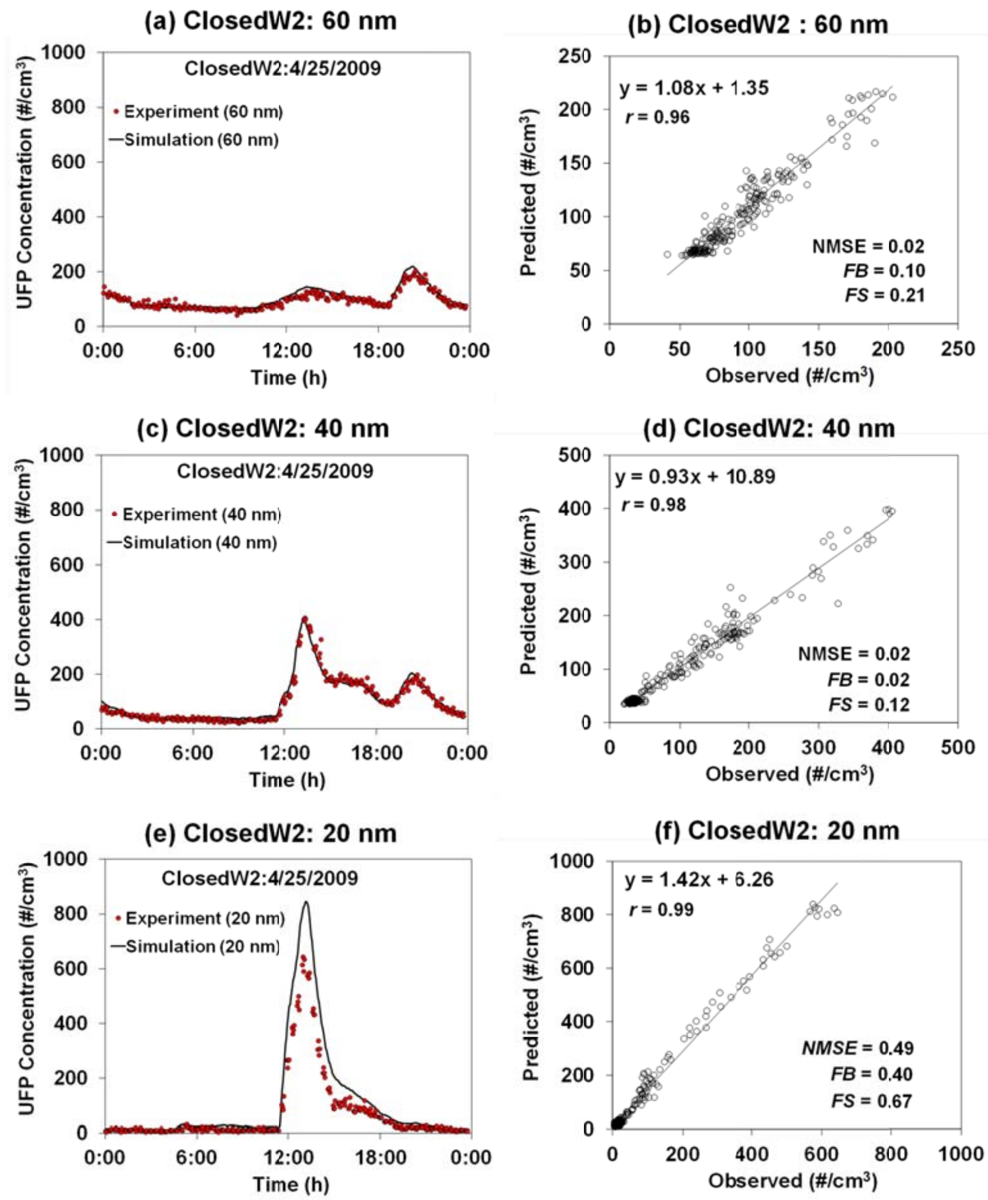

Figure 5. Comparison of measurement and model prediction for number concentrations with closed windows: a-b) 60 nm; c-d) 40 nm; e-f) 20 nm. The model prediction considered both penetration and deposition losses.

Two Windows Open

Figures 6a-6d show measurement and simulation results with two windows open (2WinOpn4). Similar to the behavior for the closed window condition, the indoor-outdoor concentration relationships vary with particle size. Comparison of the different simulation results (A, B and C) demonstrates that nearly 100 % outdoor particles penetrate into the building through open windows. This result implies that when a building is operated with open windows, deposition plays a major role in particle loss within a building and the UFP transport model needs to include reliable deposition rates to predict indoor concentrations with reasonable accuracy. As long as the model predicts the average air change rate within an acceptable range of accuracy, the deposition rate is the most important input for prediction of temporal indoor-outdoor UFP transport under open-window conditions. This is especially true when the central fan is operating and deposition rate is high within the building.

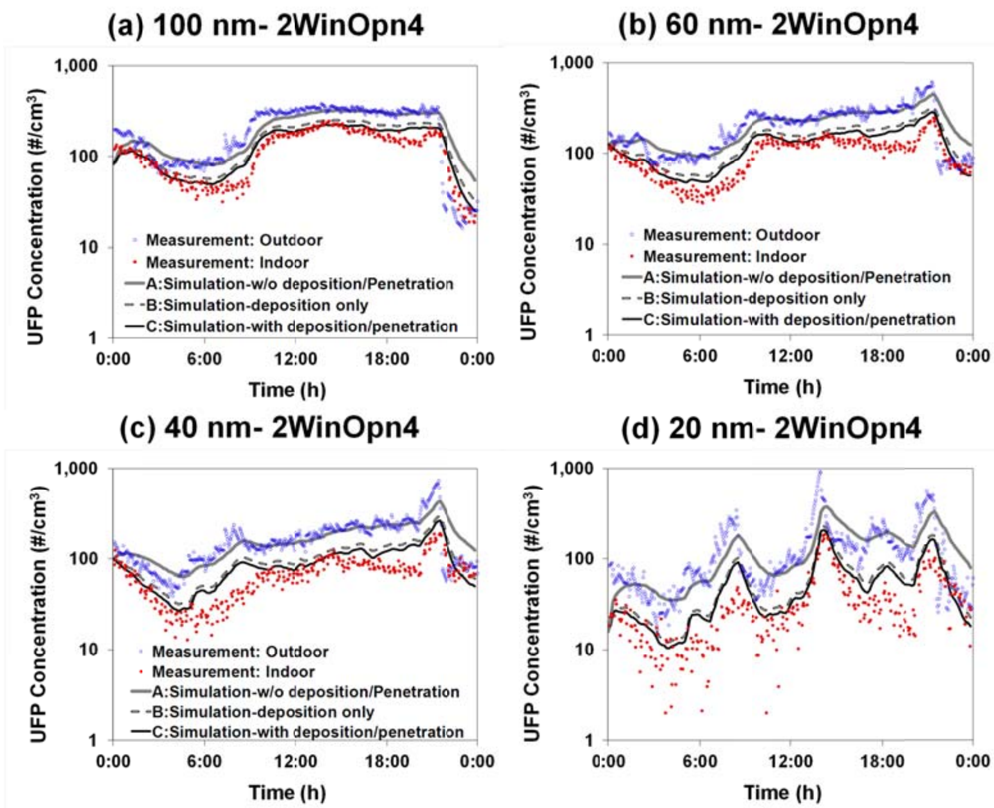

Figure 6. Time-varying (24-h) particle concentration profiles – measurement and simulation for the test 2WinOpn4: (a) 100 nm, (b) 60 nm, (c) 40 nm, and (d) 20 nm. The simulation results are varied depending on the consideration of penetration and deposition.

Figures 7a-7f compare the model predictions and measurements for two-window open conditions. The figures show that the predictions match the measurements of time-varying indoor concentration well even though there are small discrepancies in local peaks. These discrepancies might occur due to airflow effects such as increased momentum effect and turbulent fluctuation of the flow around the building that are not considered in the CONTAM model. It is also possible that the particle deposition rate changes over time during the experiment because of temporal variation in indoor airflow, while the model uses constant deposition rates. However, the simulation-to-experiment comparisons in Figure 7 show that relative differences are small and the model can predict the overall trend of the time-varying UFP concentration.

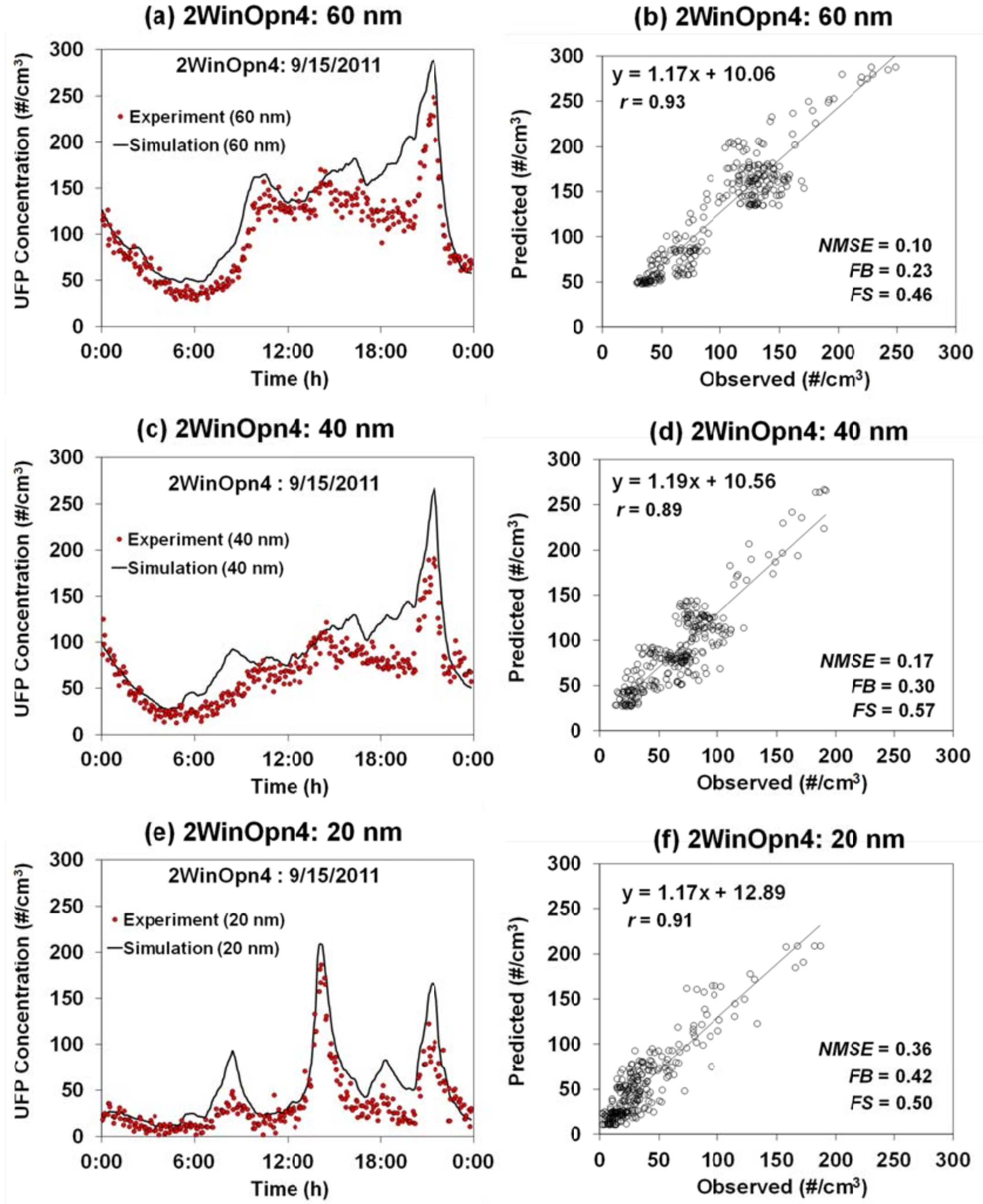

Figure 7. Comparison of measurement and model prediction for number concentrations with two windows open: a-b) 60 nm; c-d) 40 nm; e-f) 20 nm The model predictions consider both penetration and deposition losses.

Table S3 (See Supplementary Material) provides details of statistical analyses based on ASTM D5157 (ASTM 2003) for the comparison of measurements and model predictions of time-varying UFP concentrations. In the table, the first three statistical parameters (r, *M*, and b/C_{avg}) characterize the accuracy of the model predictions, and next three additional parameters (*NMSE,* |*FB*|, |*FS*|) assess bias and variance. The statistical analyses show that the agreement between observation and model prediction is not perfect for all the test cases. However, it is encouraging to note that many of the statistical parameters are in the acceptable range. For instance, in most of the cases with closed windows, the model predicts total UFP concentrations with acceptable accuracy without bias. The multi-zone model was able to capture temporal variations in UFP concentrations including the peak levels and timing under many of conditions of varying weather and window opening area.

Indoor-Outdoor Concentration Relationship

Figure 8 summarizes 24-h average indoor-outdoor (I-O) concentration ratios observed and simulated for three different particle sizes (20 nm, 60 nm, and 100 nm) and total UFP (3 nm to 100 nm) under different window opening conditions. The figure suggests that I-O ratio for UFP number concentration is a strong function of particle size and window operation. For the three particle sizes considered, the 24-h average I-O ratio ranges from 0.09 to 0.22 for closed window, from 0.13 to 0.65 for one window open, and from 0.41 to 0.66 for two windows open. The larger I-O ratios observed with open windows indicate that high indoor concentrations of outdoor ultrafine particles for buildings operated with open windows. For all window operating conditions, I-O ratio increases with particle sizes, indicating that the bigger the particles, the larger fraction of the outdoor particles penetrate and remain airborne indoors. Comparing the measurement and simulation results of 24-h average I-O ratio, the percent differences are less than 12 % for closed windows, between 0 % and 62 % for one window open, and between 2 % and 30 % for two windows open. The simulation predicts UFP infiltration with a greater accuracy for the all windows closed condition, while the prediction is less accurate for open window conditions. In particular, with one window opening, the indoor-to-outdoor relationship is highly variable due to varied inward and outward airflow rates within one opening depending on wind and temperature conditions. A study by Hussein et al. (2005) also found higher variability of I-O ratio under open window conditions than closed window conditions. Nonetheless, the simulation results provide useful insight into the relationship between indoor and outdoor UFP concentrations.

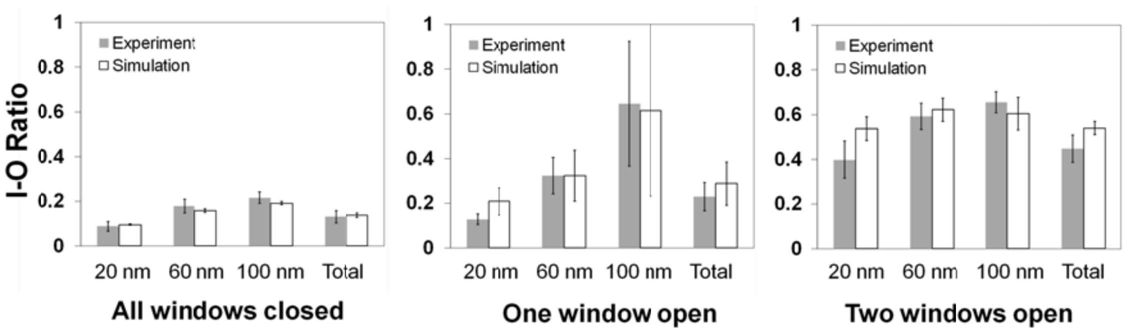

Figure 8. Indoor-outdoor (I-O) ratio for three different window operation modes: all windows closed, one window open, and two windows open. Measurement vs. simulation results are reported for 20 nm, 60 nm, 100 nm, and total UFP (3-100 nm). Error bars represent standard error from the mean obtained from multiple tests.

It should be noted that the parameters applied to model the indoor-outdoor UFP transport likely differ for other U.S. homes and buildings. The variations in penetration coefficient and deposition rate among buildings affect the overall performance of using CONTAM to evaluate indoor-outdoor UFP dynamics in buildings. In this context, some parametric test cases were considered in which deposition rate and penetration coefficient vary ±30% around the value used in the simulations discussed previously. Table 3 suggests that the effects of penetration and deposition are equally important for the case with closed-window, while deposition has more significant effects for the case with open-window. Comparing the different sizes of particles, variation in penetration coefficient has larger effects for bigger particles, whereas variation in deposition rate has larger impacts for smaller particles. These results imply that future studies should consider the variations in penetration and deposition as a function of particle size to study indoor-outdoor UFP dynamics in buildings.

Table 3. Sensitivity analysis for two test case cases: closed windows (ClosedW2) and two windows open (2WinOpn4).

Variations in *P* and *k*		% Increase in Average I-O Ratio							
		Closed Windows ClosedW2 (4/25/09)				***Two Windows Open*** 2WinOpn4 (9/5/11)			
		20 nm	40 nm	60 nm	100 nm	20 nm	40 nm	60 nm	100 nm
P	30 % increase	10	16	19	27	3	4	4	6
	30 % decrease	-9	-14	-18	-21	-3	-4	-5	-6
k	30 % increase	-18	-16	-14	-13	-14	-10	-8	-6
	30 % decrease	28	23	21	17	18	12	10	7

Study Limitations and Implications

This study presents new and important information demonstrating the ability to predict indoor UFP levels arising from outdoor variations in concentration for different window positions. However, a number of important limitations in the present study need to be noted that merit additional study in the future. The multi-zone model assumed that outdoor concentrations were spatially uniform around the building, while the measurement of outdoor UFP concentration was performed at only one façade of the test building. The model did not take into account the variability of outdoor concentrations around the building and their influence on the indoor concentrations. In addition, the multi-zone model might not capture the instantaneous momentum effects of wind through the window openings, which is particularly important under high wind speeds with open window(s).

The present study used the experimental data (a total of 12 separate measurements) mainly for model validation purpose. The measurement data were collected from a real manufactured test house under various outdoor weather and building operating conditions. As model inputs, this study used average measurement values of penetration and deposition rates. However, the penetration and deposition data used in this study are not necessarily representative of US homes in general. The penetration and deposition parameters can vary depending on the season, weather, building type, and building operating conditions (Kearney et al. 2011; Long et al.

2001). However, the CONTAM model is capable of analyzing the effect of each model input parameter on the prediction of indoor-outdoor UFP dynamics. This study provides an initial sense of the sensitivity of the predictions by varying deposition rate and penetration coefficient. A follow-up study with a larger number of US homes could address the impacts of variations in building characteristics and weather conditions, as well as their effects on penetration and deposition.

CONCLUSION

Given the challenges in measuring airborne particle transport into buildings under varied building operation and weather conditions, the present study investigated the ability of a multi-zone model to predict the entry of size-resolved outdoor ultrafine particles into a test building. CONTAM simulations and experimental studies were performed for a residential test building under three different ventilation scenarios. The results show that the model needs to consider both size-resolved deposition and penetration to predict accurately the time-varying particle concentrations in buildings. Particle deposition and penetration have significant effects in the model prediction for closed window condition, while deposition is more important than penetration for open window condition. For open window cases, the filtering effect of the building envelope decreases as relatively more of outdoor particles entry the building through the open windows. The study results also show that indoor–outdoor concentration ratio varies with particle size and building operating conditions. The model validation and statistical analyses results indicate that CONTAM model can provide insight into the general trend of UFP entry into buildings under various building operating scenarios.

Disclaimer: The full description of the procedures used in this paper requires the identification of certain commercial products and their suppliers. The inclusion of such information should in no way be construed as indicating that such products or suppliers are endorsed by NIST or are recommended by NIST, or that they are necessarily the best materials, instruments, software, or suppliers for the purposes described.

REFERENCES

ASTM, 2000, Standard test method for detecting air exchange in a single zone by means of a tracer gas dilution; ASTM E741, American Society for Testing and Materials.

ASTM, 2003. Standard guide for statistical evaluation of indoor air quality models. D5157-91. American Society for Testing and Materials.

Bennett, D., Koutrakis, P. 2006. Determining the infiltration of outdoor particles in the indoor environment using a dynamic model. Journal of Aerosol Science 37, 766–785.

Bräuner EV, Forchhammer L, Moller P, Simonsen J, Glasius M, Wahlin P, Raaschou-Nielsen O, Loft S., 2007. Exposure to ultrafine particles from ambient air and oxidative stress-induced DNA damage. Environmental Health Perspective 115(8),1177-1182.

Chen, Q., 2009. Ventilation performance prediction for buildings: A method overview and recent applications, Building and Environment 44(4), 848-858.

Dols. W.S., Persily, A.K., Morrow, J.B., 2011. Model development and validation for particle release experiments in a two-story office building. NIST Technical Note 1703, National Institute of Standards and Technology, Gaithersburg, MD.

Emmerich, S. J. and S. J. Nabinger., 2000. Measurement and Simulation of the IAQ Impact of Particle Air Cleaner in a Single-Zone Building. NISTIR 6461, National Institute of Standards and Technology, Gaithersburg, MD.

He, C., Morawska, L., Gilbert, D., 2005. Particle deposition rates in residential houses. Atmospheric Environment 39(21), 3891-3899.

Hoek, G.; Kos, G.; Harrison, R.; de Hartog, J.; Meliefste, K.; et al., 2008. Indoor-outdoor relationships of particle number and mass in four European cities. Atmospheric Environment 42, 156–169.

Hu, B., Freihaut, J.D., Bahnfleth, W.P., Aumpansub, P, Thran, B., 2007. Modeling particle dispersion under human activity disturbance in a multizone indoor environment. Journal of Architectural Engineering 13(4), 187–93

Hussein, T., Hämeri, K., Heikkinen, M.S.A., Kulmala, M., 2005. Indoor and outdoor particle size characterization at a family house in Espoo–Finland, Atmospheric Environment 39(20a), 3697-3709.

Kearney, J. Wallace, L.A, MacNeill, M, Xu, X., VanRyswyk, K., You, H., Kulka, R., Wheeler, A.J., 2011. Residential indoor and outdoor ultrafine particles in Windsor, Ontario, Atmospheric Environment 45(40): 7583-7593

Kittelson, D.B., 1998. Engines and nanoparticles: a review. Journal of Aerosol Science 29 (5–6), 575–588.

Kulmala, M.H. Vehkamäki, T. Petäjä, M. Dal Maso, A. Lauri, V.-M. Kerminen, W. Birmili, McMurry, P.H., 2004. Formation and growth rates of ultrafine atmospheric particles: a review of observations, Journal of Aerosol Science, 35(2), 143-176.

Wallace, L.A., Emmerich, S.J., Howard-Reed, C., 2004. Effect of central fans and in-duct filters on deposition rates of ultrafine and fine particles in an occupied townhouse, Atmospheric Environment 38 (3), 405-413.

Lai, A.C.K., Nazaroff, W.W.,2000. Modeling indoor particle deposition from

turbulent flowonto smooth surfaces. Journal of Aerosol Science 31, 463–476.
Li, M., Wu, C., Zhao, S., Yang, Y., 2008. State-space model for airborne particles in multizone indoor environments. Atmospheric Environment 42, 5340-5349.
Liu, D.L., Nazaroff, W.W. 2001. Modeling pollutant penetration across building envelopes. Atmospheric Environment, 35, 4451–62.
Long, C. M.; Suh, H. H.; Catalano, P. J.; Koutrakis, P., 2001. Using time and size-resolved particulate data to quantify indoor penetration and deposition behavior. Environmental Science and Technology, 35 (10), 2089–2099.
Mullen, N. A., Bhangar, S., Hering, S.V., Kreisberg, N.M., Nazaroff, W.W., 2011. Ultrafine particle concentrations and exposures in six elementary school classrooms in northern California. Indoor Air 21, 77-87.
Nabinger, S.J., Persily, A.K., 2011. Impacts of airtightening retrofits on ventilation rates and energy consumption in a manufactured home. Energy and Buildings 43(11), 3059-3067.
Oberdörster, G., Stone, V., Donaldson, K., 2007. Toxicology of nanoparticles: A historical perspective. Nanotoxicology 1, 2-25.
Persily, A.K., Emmerich, S.J., 2012. Indoor air quality in sustainable, energy efficient buildings, HVAC&R Research 18(1-2), 4-20
Rim, D., Wallace, L., Persily A., 2010. Infiltration of outdoor ultrafine particles into a test house. Environmental Science and Technology, 44, 5908–5913.
Rim, D., Green, M., Wallace, L.A., Persily, A.K., Choi, J., 2012. Evolution of ultrafine particle size distributions following indoor episodic releases: relative importance of coagulation, deposition and ventilation. Aerosol Science and Technology 46 (5), 494-503.
Sohn, M.D., Apte, M.G., Sextro, R.G., Lai, C.K., 2007. Predicting Size-Resolved Particle Behavior in Multizone Buildings. Atmospheric Environment 41, 1473–1482.
Stölzel, M., Breitner, S., Cyrys, J., Pitz, M., Wolke, G., Kreyling, W., Heinrich, J., Wichmann, H.E., Peters, A., 2007. Daily mortality and particulate matter in different size classes in Erfurt Germany. Journal of Exposure Science & Environmental Epidemiology 17(5), 458-467.
Vinzents, P.S., Møller, P., Sørensen, M., Knudsen, L.E., Hertel, O., Jensen, F.P., Schibye, B., Loft, S., 2005. Personal Exposure to Ultrafine Particles and Oxidative DNA Damage. Environmental Health Perspectives 113 (11), 1485-1490.
Walton, G.N., Dols, W.S., 2005. CONTAM 2.4 User Guide and Program Documentation. National Institute of Standards and Technology, Gaithersburg, MD.
Wang L, Chen Q., 2008. Evaluation of some assumptions used in multizone airflow network models. Building and Environment. 43(10), 1671–1677.
Zhu, Y., Hinds, W. C., Krudysz, M., Kuhn, T., Fronies, J., Sioutas, C., 2005 Penetration of freeway ultrafine particles into indoor environments. Journal of Aerosol Science 36, 303–322.

Table S1. Exterior air leakage for the test building in CONTAM model.

Building Component	Effective leakage area
Exterior wall	0.11 cm^2/m^2
Exterior door (closed)	18.7 cm^2 (per unit)
Wall interface at building corners	0.63 cm^2/m^2
Garage exterior walls	2.64 cm^2/m^2
Closed windows	5.0 cm^2 (per unit)
Crawl space wall	1.43 cm^2/m^2
Floor wall	0.97 cm^2/m
Ceiling wall	0.63 cm^2/m

Table S2. Average airflow rates and fractions of the total airflow into the building through the two windows: Win1 and Win2

Window Condition	TEST ID	Average airflow rate through the two windows (Win1&Win2) (m^3/h)				Average fraction of the total airflow through the two windows (%)	
		Inward		Outward		Inward (Win1+Win2)	Outward (Win1+Win2)
		Win1	Win2	Win1	Win2		
All windows closed	ClosedW1	8.4	2.6	7.6	1.4	10	5
	ClosedW2	3.1	0.89	2.7	0.41	9	6
	ClosedW3	1.2	0.19	0.76	0.17	8	6
	ClosedW4	2.9	0.73	2.7	0.44	10	6
One window open	1WinOpn1	43	1.5	201	0	61	90
	1WinOpn2	78	0.82	46	0.88	78	75
	1WinOpn3	52	0.97	55	0.66	76	80
	1WinOpn4	85	1.1	90	0.77	70	85
Two windows open	2WinOpn1	640	510	450	503	98	98
	2WinOpn2	630	500	490	510	99	98
	2WinOpn3	190	310	311	147	97	96
	2WinOpn4	210	280	316	159	97	97

Table S3. Summary of statistical analyses based on ASTM guideline parameters (Bold numbers represent that the value is within the guideline range)

I. Closed Windows

	ClosedW1: 3/1/2009				**ClosedW2:4/25/2009**			
Criteria	20 nm	40 nm	60 nm	Total	20 nm	40 nm	60 nm	Total
$r \geq 0.9$	0.85	**0.97**	**0.95**	**0.94**	**0.99**	**0.98**	**0.96**	**0.99**
M 0.75-1.25	**0.77**	**1.02**	**1.11**	**1.20**	1.42	**0.93**	**1.08**	1.36
$b/C_{avg} \leq 0.25$	**0.01**	**0.11**	**0.09**	0.33	**0.04**	**0.07**	**0.01**	**0.11**
$NMSE \leq 0.25$	0.31	**0.05**	**0.07**	**0.10**	0.49	**0.02**	**0.02**	**0.12**
$\|FB\| \leq 0.25$	0.28	**0.10**	**0.04**	**0.18**	0.40	**0.02**	**0.10**	**0.20**
$\|FS\| \leq 0.50$	**0.20**	**0.09**	**0.28**	**0.48**	0.67	**0.12**	**0.21**	0.62

	ClosedW3: 5/2/2009				**ClosedW4:5/9/2009**			
Criteria	20 nm	40 nm	60 nm	Total	20 nm	40 nm	60 nm	Total
$r \geq 0.9$	0.76	**0.92**	**0.97**	**0.94**	**0.95**	**0.89**	0.76	**0.92**
M 0.75-1.25	0.62	**0.80**	**0.99**	**1.03**	**1.12**	**0.80**	0.46	**0.99**
$b/C_{avg} \leq 0.25$	0.40	**0.05**	**0.14**	**0.16**	**0.06**	**0.12**	0.49	**0.01**
$NMSE \leq 0.25$	**0.24**	**0.08**	**0.05**	**0.05**	**0.11**	**0.12**	**0.08**	**0.06**
$\|FB\| \leq 0.25$	**0.03**	**0.17**	**0.18**	**0.14**	**0.05**	**0.12**	**0.11**	**0.04**
$\|FS\| \leq 0.50$	**0.41**	**0.28**	**0.01**	**0.15**	**0.32**	0.85	1.12	**0.33**

II. One Window Open

	1WinOpn1: 9/21/2008				**1WinOpn2:10/4/2008**			
Criteria	20 nm	40 nm	60 nm	Total	20 nm	40 nm	60 nm	Total
$r \geq 0.9$	0.84	**0.97**	**0.97**	**0.92**	**0.97**	0.87	**0.94**	0.73
M 0.75-1.25	**0.95**	1.40	1.33	1.35	**1.08**	**0.76**	**1.07**	0.74
$b/C_{avg} \leq 0.25$	**0.25**	**0.09**	**0.07**	**0.01**	**0.08**	**0.22**	**0.05**	0.32
$NMSE \leq 0.25$	**0.19**	**0.14**	**0.09**	**0.12**	**0.08**	**0.04**	**0.03**	**0.03**
$\|FB\| \leq 0.25$	0.30	0.27	**0.23**	0.29	**0.14**	**0.01**	**0.02**	**0.05**
$\|FS\| \leq 0.50$	**0.25**	0.69	0.61	0.75	**0.20**	**0.33**	**0.27**	**0.01**

	1WinOpn3: 9/6/2009				**1WinOpn4:9/20/2009**			
Criteria	20 nm	40 nm	60 nm	Total	20 nm	40 nm	60 nm	Total
$r \geq 0.9$	0.79	0.84	**0.91**	0.84	**0.93**	**0.96**	0.87	**0.91**
M 0.75-1.25	**0.96**	0.70	1.89	**1.24**	1.52	**0.97**	**0.89**	**1.09**
$b/C_{avg} \leq 0.25$	0.34	**0.08**	0.58	**0.09**	**0.01**	**0.13**	**0.13**	**0.08**
$NMSE \leq 0.25$	**0.22**	**0.09**	0.26	**0.10**	0.38	**0.04**	**0.03**	**0.06**
$\|FB\| \leq 0.25$	0.27	**0.15**	0.27	**0.05**	0.44	**0.09**	**0.01**	**0.04**
$\|FS\| \leq 0.50$	**0.38**	**0.50**	1.24	0.57	0.93	**0.01**	**0.04**	**0.33**

III. Two windows open

	2WinOpn1: 10/2/2010				**2WinOpn2:10/17/2010**			
Criteria	20 nm	40 nm	60 nm	Total	20 nm	40 nm	60 nm	Total
$r \geq 0.9$	**0.96**	**0.97**	**0.94**	**0.96**	**0.96**	**0.96**	**0.94**	**0.98**
M 0.75-1.25	**1.19**	**1.22**	**1.11**	1.30	0.74	**0.86**	**1.06**	0.74
$b/C_{avg} \leq 0.25$	0.26	**0.04**	**0.10**	**0.07**	**0.09**	**0.06**	**0.07**	**0.13**
$NMSE \leq 0.25$	**0.22**	**0.12**	**0.07**	**0.16**	**0.40**	**0.04**	**0.02**	**0.10**
$\|FB\| \leq 0.25$	0.38	**0.24**	**0.20**	0.34	**0.19**	**0.09**	**0.04**	**0.14**
$\|FS\| \leq 0.50$	**0.45**	0.51	**0.35**	0.62	0.51	**0.21**	**0.17**	0.55

	2WinOpn3: 7/15/2011				2WinOpn4:9/5/2011			
Criteria	20 nm	40 nm	60 nm	Total	20 nm	40 nm	60 nm	Total
r ≥ 0.9	**0.96**	**0.93**	**0.95**	**0.95**	**0.91**	0.89	**0.93**	0.89
M 0.75-1.25	**1.20**	**0.88**	**0.82**	**1.10**	**1.17**	**1.19**	**1.17**	**1.08**
$b/C_{avg} \leq 0.25$	**0.11**	**0.24**	**0.22**	**0.06**	**0.20**	**0.09**	**0.07**	**0.15**
NMSE ≤ 0.25	**0.24**	**0.03**	**0.02**	**0.04**	0.36	**0.17**	**0.10**	**0.17**
$\lvert FB \rvert \leq 0.25$	0.27	**0.11**	**0.04**	**0.15**	0.42	0.30	**0.23**	**0.28**
$\lvert FS \rvert \leq 0.50$	**0.44**	**0.12**	**0.**27	**0.29**	**0.50**	0.57	**0.46**	**0.40**